CLM-P586

CLM-P586

UKAEA

Preprint

THE ANALYSIS OF THE n=2 - 2 TRANSITIONS IN THE XUV SPECTRA OF Cr to Ni

K. D. LAWSON
N. J. PEACOCK

CULHAM LABORATORY
Abingdon Oxfordshire

1980

CLM-P 586

THE ANALYSIS OF THE n = 2 - 2 TRANSITIONS IN THE XUV SPECTRA OF Cr to Ni

by

K D Lawson* and N J Peacock

Culham Laboratory, Abingdon, Oxon.,OX14 3DB, UK.
(Euratom/UKAEA Fusion Association)

ABSTRACT

Over 400 new identifications of emission lines in the grazing incidence spectra of the elements from chromium to nickel are reported. The great majority of these lines belong to the $2s^n2p^k - 2s^{n-1}2p^{k+1}$ transition arrays in the OI to BeI isoelectronic sequences. Some of the spectra belonging to the NI, CI, BI and BeI sequences are identified as intercombination lines. The new data, taken together with other published results in the FI to LiI isoelectronic sequences, allows a complete listing of $2s^n2p^k - 2s^{n-1}2p^{k+1}$ transitions in the elements from chromium to nickel, with their appropriate term schemes. The term schemes lead to wavelength predictions for various forbidden transitions. The use of these allowed and forbidden transitions has been proposed by other authors for diagnostic purposes in solar flare and laboratory plasmas. In addition to the n=2-2 transitions the wavelengths of some NaI-like ions of the elements Cr to Ni are presented.

The plasma source used to obtain the spectra and to differentiate between the emission from separate ionisation stages was created by focusing the output of a 40 gigawatt neodymium glass laser system onto plane metallic targets.

Submitted to J.Phys.B: Atom.Molec.Phys.

* On attachment from Royal Holloway College, University of London.

APRIL 1979
erb

1. INTRODUCTION

In the past few years, there has been considerable interest in the identification and uses of the emission lines belonging to the $2s^n2p^k - 2s^{n-1}2p^{k+1}$ transition arrays of the elements in the fourth period of the periodic table. These lines can be seen in the XUV spectra of the elements. The initial motivation for the work of identification arose from the need to analyse solar flare spectra (Kastner et al.1974). The lines, which are only emitted by the high temperature flares, fall in a window of the quiet sun spectrum and are, therefore, ideally suited for providing both gross and detailed information about the ion abundances and plasma parameters of the flares (Feldman et al. 1979).

The identification of these transitions also allow wavelength predictions to be made of various forbidden lines which are seen in the UV and visible regions of solar flare spectra. Once identified, their intensity ratios can be used for electron density measurements (Feldman et al. 1978).

The $2s^n2p^k - 2s^{n-1}2p^{k+1}$ transitions also occur in laboratory plasmas, examples of topical interest being tokamak plasmas (Hinnov 1976, Breton et al.1979) and laser produced plasmas. In tokamak discharges, impurities from either the vacuum chamber walls (iron, chromium and nickel) or the current - aperture limiter, usually also a metal, become highly stripped, resulting in the emission of spectra containing both allowed and forbidden n=2-2 transitions. As in solar plasmas, these transitions are useful for diagnostic purposes (Suckewer and Hinnov 1978, Feldman and Doschek 1977, Feldman et al.1979).

Plasmas created by focusing the output of a laser system onto plane targets have been widely used as a source for line identification studies, as well as for testing diagnostic techniques (Doscheck et al.1975b,Peregudov et al.1978). The most important contributions to the work of identification have been made by three groups. At NRL and the Goddard Space Flight Centre, identifications of the most intense $2s^22p^k$-$2s2p^{k+1}$ transitions in the FI to BI isoelectronic sequences have been made for the elements from titanium to nickel (Doschek et al.1974, Feldman et al.1975, Doschek et al. 1975a) and, more recently, this work has been extended to include zinc and germanium (Behring et al. 1976). Kononov and co-workers have made detailed analyses of

the spectra of calcium (Kononov et al. 1975, Kononov et al. 1976b), titanium (Kasyanov et al. 1974) and iron (Kononov et al. 1976a), the latter paper discussing the identifications made by Kastner et al. (1974) in solar flare spectra. The Russian group have also extended their identifications to include higher Z elements (Kononov et al. 1977) and they report on observations of OI-like intercombination lines (Kononov et al. 1976c). Various lines in the laboratory spectra of potassium to chromium and some iron transitions in solar flare spectra have been studied by Fawcett and Hayes (1975) and Fawcett and Cowan (1975). In addition, Fawcett (1975) has collected much of the available data on these transitions into a single listing.

In the present work over 400 new identifications in the spectra of the elements from chromium to nickel are reported. Most of these lines are assigned to transitions within the $2s^n2p^k$-$2s^{n-1}2p^{k+1}$ arrays belonging to the OI to BeI isoelectronic sequences. The first laboratory observations of Li I-like transitions in chromium and manganese are also given and intercombination lines are observed for the first time in laboratory plasmas of these elements in the NI to BeI sequences. New intercombination lines are seen in the OI sequence.

A complete listing of the observed wavelengths and transitions within the $2s^n2p^k$-$2s^{n-1}2p^{k+1}$ transition arrays in the FI to Li I isoelectronic sequences is presented for the elements from chromium to nickel. Using these wavelengths, almost complete term schemes for the $2s^n2p^k$ configurations have been calculated for these elements. The schemes will allow wavelength predictions of various forbidden transitions to be made with a much greater accuracy than has hitherto been possible. In addition, wavelengths of four sequences of Na I-like, n=4-5 transitions are given. These Na I-like lines are found to be particularly intense in the Co and Ni spectra and, consequently, can lead to confusion with the n=2-2 transitions.

2. EXPERIMENTAL TECHNIQUES

The plasma source used to obtain the spectra of the elements being studied was produced by focusing the output of a neodymium glass laser system onto plane targets of the respective metals. The metals used were at least 99.99% pure. The resulting plasma plume was positioned

about 4 cm from and parallel to the entrance slit of an E580, Rank Hilger, grazing incidence spectrograph. This is a 2 metre instrument and the entrance slit, adjusted to a width of 4μm, was positioned to give an angle of incidence of about 88^{o}. A Bausch and Lomb, gold replica grating, ruled with 600 lines per mm and with a listed blaze angle of $1^{o}31'$, was used in the spectrograph. The spectra were recorded on Ilford Q2 plates.

The dependence of the degree of ionisation on the duration of the laser pulse was investigated. The output pulsewidth of the laser was varied from a nanosecond to several nanoseconds by clipping the Q spoiled output from the oscillator stage with an electro-optic shutter, while keeping the pump power level to the amplifier stages constant. The effect of increasing the pulse length under these conditions is to slowly decrease the laser output power while greatly increasing the output energy. The degree of ionisation was observed to increase with pulse duration, a value of 3.7 ns FWHM generating the highest ionisation stages. Two contributory factors are suggested to account for this observation. The longer irradiation pulses could give rise to an increased plasma density scale length resulting in a closer approach to stationary ionisation balance (Galanti and Peacock 1975). Alternatively, the lower intensity of the longer pulses may have improved the beam quality through a reduction in non-linear refraction and, therefore, raised the focused intensity at the target. The highest output power used was typically 40 GW, corresponding to 4×10^{14} W cm^{-2} at the target surface.

Another control on the plasma temperature was the focusing of the output lens of the laser. In these experiments an aspheric, f/1.4, Soro lens was used. The position for the lens corresponding to the observation of the highest ionisation stages was determined by monitoring the laser pulse reflected from the plasma; it was found to correspond to the maximum intensity of this reflected pulse. However, as the optimum focusing position was approached it was also found that the spectral lines became significantly weaker. In many cases, this necessitated taking multiple exposures of up to twelve irradiation pulses.

By adjusting the focusing of the Soro lens and the laser output power, spectra at various temperatures were taken of each of the five elements. As the temperature was increased, additional ionisation stages were observed and it was possible to determine the precise ionisation stage of the majority of the spectral lines. This information greatly simplified the anlysis. Figure 1 shows high temperature spectra of chromium, iron and nickel and figure 2 illustrates the change in the nickel spectrum as the temperature is varied. The resolution of the low temperature spectra was better than 1 in 3000 at 100 Å; however, as can be seen in figure 2 there is significant broadening of the spectral lines as the temperature is increased.

3. SPECTRAL CLASSIFICATIONS

The wavelength predictions for the allowed n=2-2 transitions were made by graphical extrapolations along isoelectronic sequences of the differences between the wavenumbers of consecutive elements. When a sufficient number of transitions had been identified, further predictions were made by applying the Ritz combination principle. Theoretically, the wavenumbers of isoelectronic sequences of $\Delta n=0$ transitions vary linearly with Z (Edlén 1964). Although significant deviations from a linear behaviour were found, this method still proved to be a sensitive technique for predicting the wavelengths of these transitions. The accuracy of the predictions varied considerably, depending on the interval over which the extrapolation was made. For some transitions in the CI to Li I sequences it was necessary to extrapolate from calcium. In the worst of these cases the prediction was found to differ by about 2 Å from the observed wavelength; the ability to determine the precise ionisation stages of the lines in the appropriate spectral region proved to be invaluable. Once the identifications in chromium were completed, the accuracy of the predictions in the heavier elements was greatly improved and further identifications in manganese and iron resulted in the predictions in cobalt and nickel being within 0.15 Å of the observed wavelengths. In making these identifications, much use was made of the observed relative line intensities of lower Z elements reported by other authors.

In the case of the intercombination lines, the OI isoelectronic sequences were identified by extrapolating from the wavelengths of the

$2s^2 2p^4\ ^3P - 2s2p^5\ ^1P_1$ transitions observed by Kononov et al.(1976c) in iron, nickel, copper and zinc and by using the Ritz combination principle. In the other sequences the wavelengths of the intercombination lines were predicted using the energy levels calculated by Fawcett (1975) and the combination principle and extrapolations, where necessary. The accuracy of the intercombination predictions in the NI sequence was found to be about 2 Å for lines in the spectral region around 100 Å. In the CI and Be I sequences the predictions were found to be better, being accurate to, respectively, 0.1 Å and 0.4 Å in the same region of the spectrum. The BI sequence will be discussed in more detail in section 3.6. Predictions for the $2s2p^3\ ^5S_2 - 2p^4\ ^3P_2$ transition in the CI sequence were made using solar flare data given by Dere (1978).

The wavelength calibration of the spectra was based on previously published wavelengths of n=2-2 transitions. Discrepancies between different authors and with the present measurements indicate an accuracy of ± 0.03 Å below 180 Å and ± 0.06 Å above this wavelength. It is expected that in many cases, however, the accuracy is better than these values.

The wavelengths and line intensities of the four sequences of NaI-like lines and all the observed transitions within the $2s^n 2p^k - 2s^{n-1} 2p^{k+1}$ arrays in the elements from chromium to nickel are listed together with their classifications in Tables 1 - 8. In Tables 9 - 15 the term schemes of the $2s^n 2p^k$ configurations for these elements are given. LS coupling notation is used to describe the energy levels. This is both because of its simplicity and its use throughout the literature in connnection with these transitions. However, it should be emphasised that,in these high Z elements,there is considerable mixing of the electron states and a more appropriate description would be given by intermediate coupling notation. Evidence for the mixing of some states in the OI and Be I sequences is presented in section 3.3 in terms of the 'anomalous' variation of their transition energies with nuclear charge. The S-D and D-S forbidden transitions observed in the NI and BI sequences are thought to result from this state mixing.

The line intensities listed with each wavelength are based on a

scale from 1 to 11 which is fixed by giving the $2s^2 2p^5\ ^2P_{3/2} - 2s2p^6\ ^2S_{\frac{1}{2}}$ transition in each element an intensity of 10. In cases where blending might result in a misleading intensity, this is indicated by the letter 'a'. For some lines, the blending has also made it difficult to measure wavelengths to an accuracy better than the wavelength spread of the blend and wavelengths have been calculated from the derived term schemes. All such wavelengths are entirely consistent with the extrapolations and measurements of the spectra; they are denoted by the letter 'b'.

The accuracy of the energies given in the term schemes is about $\pm$ 250 cm^{-1}, there being greatest uncertainty in the energies of those levels defined by only one transition.

3.1. NaI SEQUENCE

The wavelengths of four sequences of Na I-like lines are given in Table 1. These lines are found to be intense in the present spectra, particularly in cobalt and nickel, and, consequently, their identifications are presented so as to avoid possible confusion with the n=2-2 transitions. The lines correspond to $2p^6 4f - 2p^6 5g$ and $2p^6 4d - 2p^6 5f$ transitions. In each case the long wavelength member of the multiplet is too weak to be seen. Wavelength predictions for the 4f-5g transitions were obtained from extrapolations of the data given by Kononov et al.(1977). Those for the 4d-5f transitions in iron and nickel were calculated by the Hartree-X computer code (Cowan and Griffin 1976), the discrepancies between predicted and observed wavelengths being smaller than 0.2 Å. Extrapolation of the wavenumber differences between consecutive elements was used to derive the remaining wavelengths.

3.2. FI SEQUENCE

The emission lines belonging to the FI sequence, an intense doublet, have already been identified by other authors in all the elements considered. For completeness, they are listed in Table 2 and the term schemes are given in Table 9.

3.3. OI SEQUENCE

The allowed transitions in this sequence are well known and intercombination lines identified with the $2s^2 2p^4\ ^3P - 2s2p^5\ ^1P_1$

transitions have been reported by Kononov et al. (1976c). It has been possible to complete the $^3P - {}^1P_1$ sequences and identify other sequences of intercombination lines. The identifications and term schemes are presented in tables 3 and 10, respectively.

In this sequence, two of the isoelectronic extrapolation curves used for predicting wavelengths were found to have an atypical behaviour. In general, the extrapolation curves of the wavenumber differences of consecutive elements are similar in shape to that of the $2s^22p^4\ {}^3P_1 - 2s2p^5\ {}^3P_1$ transition shown in figure 3. For a few longer wavelength transitions the curves are as for the Be I-like $2s2p\,{}^3P_2 - 2p^2\ {}^3P_2$ transition, illustrated in the same diagram. The extrapolation curves associated with the $2s^22p^4\ {}^1S_o - 2s2p^5\ {}^1P_1$ and $2s^22p^4\ {}^3P_o - 2s2p^5\ {}^3P_1$ transitions, shown in figure 4, exhibit a quite different behaviour, the former curve showing a definite maximum within the range of elements studied and the latter rising more steeply than "normal" at high Z. The reason for the rapid divergence of these curves at high Z is attributed to mixing between the $2s^22p^4\ {}^1S_o$ and the other level of equal J within the same configuration, the $2s^22p^4\ {}^3P_o$ level (Kononov 1978). Computational results suggest that the energy of the upper levels of each of the transitions vary smoothly with Z and, consequently, the extrapolation curves give a fairly sensitive indication of the movement of the lower energy levels.

A similar effect is observed in the BeI sequence between the $2s2p\,{}^3P_1 - 2p^2\ {}^3P_o$ and $2s2p\,{}^1P_1 - 2p^2\ {}^1S_o$ transitions. The extrapolation curves are illustrated in figure 5. It can be seen that, in this case, it is the $2s2p\,{}^3P_1 - 2p^2\ {}^3P_o$ curve which has a maximum and the $2s2p\,{}^1P_1 - 2p^2\ {}^1S_o$ curve a steep rise. Again strong mixing of the $2p^2\ {}^3P_o$ and $2p^2\ {}^1S_o$ levels is responsible for the divergence of the transition energies at high Z.

3.4.NI SEQUENCE

On the whole, good agreement has been found with previously published identifications and it has been possible to extend these identifications to include other elements and other sequences of transitions. There was no evidence, however, of lines corresponding to the $2s^22p^3\ {}^2D_{5/2} - 2s2p^4\ {}^2D_{3/2}$ transition in any of the spectra and this brings into question the identification of this transition in iron (Kononov et al.1976a).

The forbidden $2s^2 2p^3\ ^2D_{3/2}$ - $2s2p^4\ ^2S_{\frac{1}{2}}$ transition is seen as an intense line in these spectra. This transition and the corresponding, but weaker one in the BI sequence, the $2s2p^2\ ^2S_{\frac{1}{2}}$ - $2p^3\ ^2D_{3/2}$ transition, are thought to be a result of the mixing of energy levels with equal J.

Sequences of NI-like, n=2-2 intercombination lines have been seen for the first time in laboratory plasmas. Using these identifications, it is possible to predict the wavelengths of the $2s^2 2p^3(^4S_{3/2}$ - $^2P_{3/2})$ and $2s^2 2p^3(^4S_{3/2}$ - $^2P_{\frac{1}{2}})$ forbidden lines; in iron, the predicted wavelengths are, respectively, 309.4 ± 0.2Å and 384.5 ± 0.4Å. However, there is a discrepancy between these values and the identifications of the transitions at 326.76Å and 411.61Å in solar flare spectra (Widing 1978), this bringing the identifications into question. Predictions for the various forbidden lines seen in solar flare spectra can be calculated from the term schemes, which are given in Table 11. Table 4 lists the observed wavelengths and identifications for this sequence.

3.5. CI SEQUENCE

It has been possible to add a significant number of new identifications to the list of published transitions in this sequence, particularly for the elements cobalt and nickel. A sufficient number of transitions within the troublesome $2s2p^3$ - $2p^4$ array, many of whose lines are weak and blended, have been identified to allow a confident determination of the splittings within these configurations. CI-like, n=2-2 intercombination lines have been observed for the first time in laboratory plasmas of high Z elements. The classifications and term schemes are presented in Tables 5 and 12, respectively.

In this sequence, several discrepancies have been found with the work of other authors. Wavelengths of, respectively, 108.12 Å and 117.51 Å, for the $2s^2 2p^2\ ^3P_o$ - $2s2p^3\ ^3P_1$ and $2s^2 2p^2\ ^3P_1$ - $2s2p^3\ ^3P_1$ transitions in iron, are preferred to the values of 108.45 Å and 117.89 Å reported by Kononov et al. (1976a). This redefining of the $2s2p^3\ ^3P_1$ level has allowed the $2s^2 2p^2\ ^3P_2$ - $2s2p^3\ ^3P_1$ transition, as well as two $2s2p^3\ ^3P_1$ - $2p^4\ ^3P$ transitions, to be identified. These alternative assignments affect the identifications which Kononov et al. propose for the solar flare spectra reported by Kastner et al. (1974). It has not been possible to give an alternative identification for the solar flare line at 117.81 Å, which Kononov et al. identified with the $^3P_1$ - $^3P_1$ transition. A comparison between different flare spectra of the intensity of the line at 108.37 Å, identified

as a blend between the $2s^2 2p^4\ ^3P_2$ - $2s2p^5\ ^3P_2$ and $2s^2 2p^2\ ^3P_0$ - $2s2p^3\ ^3P_1$ transitions, suggests that this line is either entirely Fe XIX or is blended with a transition of a lower ionisation stage.

The $2s2p^3\ ^3D_1$ - $2p^4\ ^3P_0$ sequence in the elements from potassium to chromium, identified by Fawcett and Hayes (1975), does not fit an extrapolation curve from lower Z elements. For this transition in chromium, a wavelength of 118.31 Å is preferred to the value of 118.81 Å given by Fawcett and Hayes. The iron line at 125.29 Å, which has been assigned to the $2s2p^3\ ^1P_1$ - $2p^4\ ^1S_0$ transition (Kononov et al.1976a), better fits the prediction for the $2s2p^3\ ^3P_2$ - $2p^4\ ^3P_1$ transition; an alternative identification for the $2s2p^3\ ^1P_1$ - $2p^4\ ^1S_0$ transition is 127.04 Å.

As in the NI sequence, there are discrepancies between the predicted wavelengths of forbidden lines calculated from the present term schemes and identifications made in solar flare spectra. Widing (1978) identifies lines at 567.76 Å and 330.23 Å with, respectively, the $2s^2 2p^2(^3P_1$ - $^1D_2)$ and $2s^2 2p^2(^3P_1$ - $^1S_0)$ transitions in iron, whereas our predictions for these transitions are 588.1 ± 0.9Å and 336.0 ± 0.3Å. Again, this brings into question the identifications made in the solar flare spectra.

3.6. BI SEQUENCE

Apart from the identifications made by Kononov et al.(1976a) in iron, very few BI-like transitions have previously been observed in the elements from chromium to nickel. This reflects the difficulty of exciting these very highly ionised species. However, in our irradiation experiments, it has been possible to excite the BI-like ions strongly, and, consequently, a number of new identifications have been made. Two discrepancies have been found between the present identifications and those of Kononov et al. An assignment of the weak $2s2p^2\ ^2S_{\frac{1}{2}}$-$2p^3\ ^2P_{\frac{1}{2}}$ transition in iron to a line at 139.64 Å, instead of at 139.82 Å, allows three other $2s2p^2$ - $2p^3\ ^2P_{\frac{1}{2}}$ transitions to be identified, in addition to giving a better fit to the extrapolation curve. Also, the $2s2p^2\ ^2D_{5/2}$ - $2p^3\ ^2D_{3/2}$ transition in iron, which we identify with a line at 157.03 Å, appears to have been confused with the Na I-like, 4f-5g doublet at 156.80 Å and 156.88 Å. There is strong evidence for the identification of the Na I-like doublet throughout the isoelectronic sequence, since the doublet structure can be clearly resolved in all but the highest temperature spectra.

In addition to the lines identified with allowed transitions, a sequence of BI-like lines has been observed which cannot be assigned to any forbidden transition within the doublet or quartet systems. This sequence has

tentatively been identified with the $2s2p^2\ ^4P_{5/2} - 2p^3\ ^2D_{5/2}$ transition. It was more difficult to make reliable wavelength predictions for the intercombination lines by isoelectronic extrapolation of the data listed by Fawcett (1975), since the energy levels for the quartet system are only available for the elements up to phosphorous. To estimate the relative positions of the quartet and doublet systems, extrapolations were, therefore, carried out for four isoelectronic sequences of transitions and an extrapolation of the differences between the theoretical and observed values of the energies of the $2p^3\ ^4S_{\frac{1}{2}}$ level was also made. The theoretical energies were calculated from the known energies of the $2p^3\ ^2P$ and $2p^3\ ^2D$ levels using the following expressions for the interaction energies of the respective levels (Edlén 1964):-

$2p^3\ ^2P$: 3Fo

$2p^3\ ^2D$: 3Fo - $6F_2$

$2p^3\ ^4S$: 3Fo - $15F_2$

The mean and standard deviation of the results of all five extrapolations led to wavelength predictions of, respectively, 95 ± 5 Å and 99 ± 5 Å for the $2s2p^2\ ^4P_{5/2} - 2p^3\ ^2D_{5/2}$ and $2s2p^2\ ^4P_{5/2} - 2p^3\ ^2D_{3/2}$ transitions in Ni. These are the only predictions close to the observed line at 98.40 Å. Both of these transitions are expected to have relatively high gf values within the $^4P - ^2D$ multiplet, so an identification with either transition would be reasonable.

Independent predictions, obtained when additional corrections are applied to the Froese Fischer multi-configurational Hartree Fock computer programme, favour the identification of this sequence with the $^4P_{5/2} - ^2D_{5/2}$ transition (Dankwort and Trefftz 1978). Their results infer predictions of 122.4Å and 109.4 Å for this transition in chromium and iron, respectively; the observed lines are at wavelengths of 122.29Å and 109.54Å in these elements. Tentative assignments of $2s^22p^2P - 2s2p^2\ ^4P$ transitions in solar flares (Sandlin et al. 1976), based on further independent predictions, again, favour this identification. However, there is a small discrepancy between the results of Sandlin et al. and the present identifications, which has not been resolved, the former predicting a wavelength for the $^4P_{5/2} - ^2D_{5/2}$ transition in iron of 109.45 Å as compared with the observed value of 109.54 Å. This discrepancy, although small, is much larger than the expected accuracy of the present measurements and would result in greater discrepancies at the longer wavelengths of the forbidden lines, which fall in the 200 - 350 Å region of the spectrum. In the term schemes, given in Table 13, the tentative nature of this assignment is indicated by the addition of an error, x, to the quartet energy levels. The observed wavelengths for this sequence are listed in Table 6.

3.7. BE I SEQUENCE

Only two previous laboratory observations of Be I-like transitions have been made in these elements. Consequently, it was possible to make a significant contribution to the identifications within this sequence, all the allowed transitions being identified.

A sequence of intense intercombination lines was observed, which was satisfactorily identified with the $2s2p\,^3P_2 - 2p^2\,^1D_2$ transition. It appears that, with increasing Z, the upper level of this transition preferentially decays to the $2s2p\,^3P_2$ level, instead of the expected $2s2p\,^1P_1$ level, since the $2s2p\,^1P_1 - 2p^2\,^1D_2$ transition is found to be weak in these elements. Good agreement is found with the observations of the $2s^2\,^1S_o - 2s2p\,^3P_1$ transition in solar flare spectra, which for chromium and iron is reported by Widing (1975) and for manganese by Sandlin et al. (1976). Table 7 contains a list of the observed wavelengths with their classifications. The term schemes are presented in table 14, the letter x indicating a possible error due to the tentative identification of the $2s2p\,^3P_1 - 2p^2\,^3P_o$ transition in nickel.

3.8. Li I SEQUENCE

Emission lines in the Li I sequence are observed weakly in the chromium, manganese and iron spectra. The absence of these lines from the cobalt and nickel spectra is due both to the extreme difficulty of exciting these very high ionisation stages and to the long wavelength of these transitions, which occur in a spectral region where the grating efficiency is low. Despite the low intensity of the lines making the analysis less certain, a comparison with identifications made in solar flare spectra (Widing and Purcell 1976) confirmed four of the identifications made. The present wavelength of 191.99 Å for the $^2S_{\frac{1}{2}} - {}^2P_{3/2}$ transition in iron is preferred to the published value of 192.14 Å (Fawcett 1975), since it is in better agreement with the solar flare data and results in a smoother extrapolation curve. The sequences, whose wavelengths are given in Table 8, are completed with solar flare observations (Sandlin et al. 1976) and two reliable predictions. The term schemes are presented in Table 15.

4. DISCUSSION

Apart from a few minor discrepancies, previous identifications in laser-produced and solar flare plasmas of the $2s^n2p^k - 2s^{n-1}2p^{k+1}$

transitions are in good agreement with our data. Very recently, some of these transitions have also been observed in the TFR-600 tokamak (Breton et al. 1979). About twenty of these tokamak lines are new and their identifications have formed part of our present study. Where there is agreement between our data and the tokamak spectra, this is noted in the appropriate table. However, a majority of the new tokamak identifications, mostly in the higher ionisation stages of nickel, show significant discrepancies with our results.

Although we have widely used isoelectronic extrapolation as a simple method for extending wavelength predictions to neighbouring elements of higher and lower nuclear charge, the use of atomic structure codes offers some advantage when elements of widely different Z are to be considered. In addition, details of the mixing of the wave functions and estimates of the oscillator strengths can only be obtained from the theoretical models. For the $2s^n2p^k - 2s^{n-1}2p^{k+1}$ transitions, the wavelength predictions obtained from even the most sophisticated self-consistent field calculations at present available (Cowan and Griffin 1976, Froese Fischer 1972, Safronova 1975, Victorov and Safronova 1977) are best used as part of a semi-empirical method. In such a method, it is usual to extrapolate the difference of the theoretical and observed wavelengths for each element along an isoelectronic sequence (Kononov 1978,Doschek et al.1974). The present results provide a good basis from which these semi-empirical extrapolations can be made. The problem of identifying the n=2-2 transitions in high Z elements is largely due to the fact that the energy splittings within the configurations are significant compared with the mean transition energies. This results in the lines within a multiplet being very widely spaced and, consequently, different multiplets overlap one another. In addition, the transition energies are such that lines from different ionisation stages occur in the same spectral region.

The reasons for the inaccuracies in the ab inito calculations are, as yet, not fully understood. Kononov (1978) suggests that the inaccuracies in the code of Safronova (Safronova 1975, Victorov and Safronova 1977) may be due to some relativistic interactions that have not been included, such as the Lamb shift. Certainly the various relativistic corrections are of prime importance in obtaining reasonable ab inito predictions in high Z elements. For example, the Hartree-X code of Cowan (Cowan and Griffin 1976), which

has relativistic corrections, gives predictions of allowed n=2-2 transitions in the NI sequence between the elements of titanium and nickel which are typically six times closer to the observed values than those given by a non-relativistic form of the multi-configurational Hartree Foœk code of Froese Fischer (1972). Dankwort and Trefftz (1978), Glass (1979) and Bogdanovich et al.(1978) all make comparisons between the results of codes with relativistic corrections and experiment.

The computer codes calculate the energy levels within a configuration. Consequently, any errors in these calculations will be more significant for $\Delta n=0$ than $\Delta n\neq 0$ transitions, since, for the former, the error is a larger fraction of the transition energy. It follows that the codes will give poorer predictions for $\Delta n=0$ transitions and, conversely, these transitions will provide a more sensitive test for improved theoretical models. The $2s^n2p^k - 2n^{n-1}2p^{k+1}$ transitions are particularly suited for such a comparison, since wavelengths are now known for the majority of the transitions throughout an extended sequence of elements.

5. CONCLUSIONS

In this paper,we present many new identifications of both allowed and forbidden transitions within the $2s^n2p^k - 2s^{n-1}2p^{k+1}$ transition arrays in the OI to BeI isoelectronic sequences of the elements from chromium to nickel. The forbidden lines are in most cases intercombination lines, which in the NI to Be I isoelectronic sequences are identified for the first time in the laboratory spectra of high Z elements. Spectra taken at various plasma temperatures have allowed the precise ionisation stage of the majority of spectral lines to be determined. This, together with the self-consistency of the term schemes and the satisfactory extrapolation curves which fit the published data for lower Z elements, gives confidence in the new identifications.

The results will facilitate the identifications in solar flare, tokamak and other laboratory spectra of both allowed and forbidden transitions belonging to the $2s^n2p^k - 2s^{n-1}2p^{k+1}$ transition arrays and the forbidden transitions within the $2s^22p^k$ ground configurations in the elements from chromium to nickel. Such lines, once identified, will be useful for plasma diagnostic purposes. The results will also form a useful basis from which wavelength predictions in both lower and higher Z elements can be made and as data for comparison with improved theoretical models.

ACKNOWLEDGMENTS

The authors wish to acknowledge the invaluable assistance of A H Jones in modifying and operating the laser system. We would also like to thank H Gordon, M W D Mansfield and C C Smith for useful discussions during this work and, in addition, H Gordon for assistance in running the Hartree-X Computer code.

APPENDA

1) A revised copy of Breton et al.(1979) shows closer agreement with the present results than is indicated in tables 4 - 7.

2) Isoelectronic extrapolations of the $2s^2 2p\ ^2P_{3/2} - 2s2p^2\ ^4P_{\frac{1}{2}}$ transition predicted from the energy levels given in table 13 and those levels listed by Fawcett (1975) confirms the identification of the boron-like sequence of intercombination lines with the $2s2p^2\ ^4P_{5/2} - 2p^3\ ^2D_{5/2}$ transition. The correct term scheme is therefore obtained by putting x = 0 in table 13.

REFERENCES

W E BEHRING, L COHEN, G A DOSCHEK and U FELDMAN, 1976, J.Opt.Soc.Am., 66, pp 376-378

P O BOGDANOVICH, G V MERKELIS, Z B RUDZIKAS, S D ŠADŽIUVIENE and U I SAFRONOVA, 1978, Physica Scripta, 17, pp 549-555

V A BOIKO, Yu P VOINOV, V A GRIBKOV and G V SKLIZKOV, 1970, Opt. Spectrosc., 29, pp 545-546

C BRETON, C DeMICHELIS, M FINKENTHAL and M MATTIOLI, 1979, Euratom Report No. EUR-CEA-FC-989

R D COWAN and D C GRIFFIN, 1976, J.Opt.Soc.Am., 66, pp 1010-1014

W DANKWORT and E TREFFTZ, 1978, Astron.Astrophys., 65, pp 93-98

K P DERE, 1978, Astrophys.J., 221, pp 1062-1067

G A DOSCHEK, U FELDMAN, R D COWAN and L COHEN, 1974, Astrophys. J., 188, pp 417-422

G A DOSCHEK, U FELDMAN and L COHEN, 1975a, J.Opt.Soc.Am., 65, pp 463-464

G A DOSCHEK, U FELDMAN, J DAVIS and R D COWAN, 1975b, Phys.Rev.A, 12, pp 980-986

B EDLÉN, 1964, Encyclopaedia of Physics (S Flügge, ed.), 27, pp 80-220

B C FAWCETT, 1971, J.Phys. B, 4, pp 981-985

B C FAWCETT, 1975, Atomic Data and Nuclear Data Tables, 16, pp 135-164

B C FAWCETT and R D COWAN, 1975, Mon.Not.R.astr.Soc., 171, pp 1-8

B C FAWCETT and R W HAYES, 1975, Mon.Not.R.astr.Soc., 170, pp 185-197

B C FAWCETT, M GALANTI and N J PEACOCK, 1974, J.Phys.B, 7, pp 1149-1153

U FELDMAN and G A DOSCHEK, 1977, J.Opt.Soc.Am., 67, pp 726-734

U FELDMAN, G A DOSCHEK, D J NAGEL, W E BEHRING and L COHEN, 1973, Astrophys.J., 183, pp L43-45

U FELDMAN, G A DOSCHEK, R D COWAN and L COHEN, 1975, Astrophys.J., 196, pp 613-616

U FELDMAN, G A DOSCHEK, J T MARISKA, A K BHATIA and H E MASON, 1978, Astrophys.J., 226, pp 674-678

U FELDMAN, G A DOSCHEK, CHUNG-CHIEH CHENG and A K BHATIA, 1979, Submitted to J.Appl.Phys.

C FROESE FISCHER, 1972, Comput.Phys.Commun., 4, pp 107-116

M GALANTI and N J PEACOCK, 1975, J.Phys.B, 8, pp 2427-2447

R GLASS, 1979, J.Phys.B, 12, pp 697-703

E HINNOV, 1976, Phys.Rev.A, 14, pp 1533-1541

S O KASTNER, W M NEUPERT and M SWARTZ, 1974, Astrophys.J., 191, pp 261-270

Yu S KASYANOV, E Ya KONONOV, V V KOROBKIN, K N KOSHELEV, A N RYABTSEV, R V SEROV and E V SKOKAN, 1974, Opt. Spectrosc., 36, pp 4-6

E Ya KONONOV, 1978, Physica Scripta, 17, pp 425-432

E Ya KONONOV, K N KOSHELEV, L I PODOBEDOVA and S S CHURILOV, 1975, Opt. Spectrosc., 39, pp 458-460

E Ya KONONOV, K N KOSHELEV, L I PODOBEDOVA, S V CHEKALIN and S S CHURILOV, 1976a, J.Phys.B, 9, pp 565-572

E Ya KONONOV, K N KOSHELEV, L I PODOBEDOVA and S S CHURILOV, 1976b, Opt. Spectrosc., 40, pp 121-123

E Ya KONONOV, A N RYABTSEV, U I SAFRONOVA and S S CHURILOV, 1976c, J.Phys.B, 9, pp L477-479

E Ya KONONOV, V I KOVALEV, A N RYABTSEV and S S CHURILOV, 1977, Sov.J.Quantum Electron., 7, pp 111-112

G V PEREGUDOV, E N RAGOZINE, I Yu SKOBELEV, A V VINOGRADOV and E A YUKOV, 1978, J.Phys. D , 11, pp 2305-2311

U I SAFRONOVA, 1975, J.Quant.Spectrosc.Radiat.Transfer, 15, pp 231-242 (In Russian)

G D SANDLIN, G E BRUECKNER, V E SCHERRER and R TOUSEY, 1976, Astrophys.J., 205, pp L47-50

S SUCKEWER and E HINNOV, 1978, Phys.Rev.Lett., 41, pp 756-759

D S VICTOROV and U I SAFRONOVA, 1977, J.Quant.Spectrocs.Radiat.Transfer,17, pp 605-611

K G WIDING, 1975, Astrophys.J., 197, pp L33-35

K G WIDING, 1978, Astrophys. J., 222, pp 735-739

K G WIDING and J D PURCELL, 1976, Astrophys.J., 204, pp L151-153

TABLE 1. CLASSIFICATIONS OF LINES ISOELECTRONIC WITH SODIUM I

Transition	Cr XIV	Mn XV	Fe XVI	Co XVII	Ni XVIII
$2p^6 4d - 2p^6 5f$					
$^2D_{3/2} - ^2F_{5/2}$	187.02 (2)	163.41 (1)	144.06 (2)	127.96 (3)	114.46 (6bl)
$^2D_{5/2} - ^2F_{7/2}$	187.30 (2a)	163.63 (3a)	144.25 (2a)	128.20 (4a)	114.74 (6)
$2p^6 4f - 2p^6 5g$					
$^2F_{5/2} - ^2G_{7/2}$	204.91 (3a)	178.61 (3a)	156.80 (2a)	138.97 (5a)	123.96 (8a)A
$^2F_{7/2} - ^2G_{9/2}$	205.01 (3)	178.69 (3a)	156.88 (4a)	139.04 (5a)	124.04 (8a)A

Wavelengths given in Å.
Relative line intensities listed in brackets after each wavelength.
a indicates possible spurious line intensity due to blending.
bl denotes blend.
A- line previously identified by Kononov et al. (1977).

TABLE 2. CLASSIFICATIONS OF LINES ISOELECTRONIC WITH FLUORINE I

Transition	Cr XVI	Mn XVII	Fe XVIII	Co XIX	Ni XX
$2s^2 2p^5 - 2s2p^6$					
$^2P_{3/2} - ^2S_{\frac{1}{2}}$	106.62 (10)BC	100.00 (10)BC	93.93 (10)AF	88.35 (10)B	83.17 (10)B
$^2P_{\frac{1}{2}} - ^2S_{\frac{1}{2}}$	115.33 (9)BC	109.35 (10)BC	103.95 (10)AF	99.02 (9)B	94.49 (10)B

Wavelengths given in Å.
Relative line intensities listed in brackets after each wavelength.
Capital letters refer to previous identifications.
A - Boiko et al.(1970)
B - Doschek et al.(1974)
C - Fawcett (1971)
D - Feldman et al.(1973)

TABLE 3. CLASSIFICATIONS OF LINES ISOELECTRONIC WITH OXYGEN I

Transition	Cr XVII	Mn XVIII	Fe XIX	Co XX	Ni XXI
$2s^2p^4$-$2s2p^5$					
$^3P_2$-$^1P_1$	89.57b(7)	84.05 (6)	78.90 (4)G	74.10 (4)	69.62 (4)G
$^3P_0$-$^1P_1$	94.49 (2)	89.03 (1)	83.89 (1)G	79.01 (2bl)	74.43b(2a)
$^3P_1$-$^1P_1$	94.69 (1)	89.59 (1)	84.89 (1)G	80.51 (1)	76.45 (1)
$^1D_2$-$^1P_1$	101.91 (9)AC	96.23 (10bl)AC	91.02 (9)E	86.19 (10)A	81.69 (9)A
$^3P_2$-$^3P_1$	116.53 (9)AC	108.76 (8)AC	101.55 (8)EF	94.94 (8)A	88.81 (9)A
$^3P_1$-$^3P_0$	120.84 (8)AC	113.30 (8)AD	106.33 (6)E	99.89 (7)A	93.91 (8)A
$^3P_2$-$^3P_2$	122.91 (11)AC	115.38 (11)AC	108.37 (10)EF	101.88 (11)A	95.85 (11a)A
$^3P_0$-$^3P_1$	125.00 (7)AC	117.25 (7)AD	109.97 (6)E	103.16 (8)A	96.79 (9)A
$^3P_1$-$^3P_1$	125.35 (8bl)AC	118.22 (6)AD	111.70 (5)E	105.72 (7)A	100.23 (7)A
$^3P_1$-$^3P_2$	132.76 (9)AC	126.09 (8)AD	120.00 (8bl)EF	114.40 (8)A	109.29 (10)A
$^1S_0$-$^1P_1$	117.20 (6)A	111.39 (5)AD	106.12 (4)E	101.39 (5a)A	97.13 (6a)A
$^1D_2$-$^3P_1$					109.44 (1)T
$^1D_2$-$^3P_2$	147.40 (2)	139.65 (3)	132.63 (4a)	126.22 (3)	120.33 (5)
$2s2p^5$-$2p^6$					
$^3P_1$-$^1S_0$	97.20 (3a)	91.90 (2)	87.02 (1)	82.48 (1)	78.28 (3a)
$^1P_1$-$^1S_0$	129.78 (6)B	122.29 (7)BD	115.42 (7bl)BD	109.14 (9bl)B	103.40 (9bl)B

Wavelengths given in Å.
Relative line intensities listed in brackets after each wavelength.
a indicates possible spurious line intensity due to blending.
bl denotes blend.
b indicates that wavelength given is calculated from term scheme.
T follows wavelength of tentative identification.
Other capital letters refer to previous identifications.
A - Doschek et al. (1974)
B - Doschek et al. (1975b)
C - Fawcett (1971)
D - Fawcett et al. (1974)
E - Feldman et al. (1973)
F - Kastner et al. (1974); identifications in solar flare spectra
G - Kononov et al. (1976c)

TABLE 4. CLASSIFICATIONS OF LINES ISOELECTRONIC WITH NITROGEN I

Transition	CrXVIII	Mn XIX	Fe XX	Co XXI	Ni XXII
$2s^2 2p^3 - 2s2p^4$					
$^4S_{3/2} - ^2P_{3/2}$	90.63 (4a)	85.41 (2)	80.51 (2)	75.87 (2b1)	71.48 (2)
$^4S_{3/2} - ^2S_{1/2}$	94.16 (1)	88.75 (1)	83.69 (1)	78.90 (2a)	74.37 (1)
$^2D_{3/2} - ^2P_{1/2}$	95.77 (7)B	89.26 (5)B	83.24 (4b1)BH	77.69 (4)B	72.52 (3)
$^2D_{3/2} - ^2P_{3/2}$	102.32 (7)B	96.24 (10b1)B	90.60 (4)BH	85.40 (5b1)B	80.55 (4)B
$^2D_{5/2} - ^2P_{3/2}$	104.98 (10)B	99.17 (9)BD	93.78 (8)BH	88.77 (9)B	84.06 (9)B
$^2P_{1/2} - ^2P_{1/2}$	105.92 (2)B	99.01 (2)B	92.63 (1)	86.66 (1)	81.04 (1)
$^2P_{3/2} - ^2P_{1/2}$	110.41 (11a)B	104.13 (9b1)B	98.38 (9b1)BH	93.00 (10b1)B	88.00 (9a)B
$^2P_{1/2} - ^2P_{3/2}$	113.99 (10b1)B	107.68 (4)B	101.83 (3)BH	96.36 (3)	91.20 (4)
$^2P_{3/2} - ^2P_{3/2}$	119.21 (6)B	113.75 (4)B	108.83 (4)BH	104.27 (4)	100.12 (5a)
$^2D_{3/2} - ^2S_{1/2}$	106.84 (7)F	100.50 (6)F	94.64 (5)FH	89.25 (7)	84.24 (6)
$^4S_{3/2} - ^2D_{3/2}$	108.37 (2)	101.92 (1)	95.95 (2)	90.31 (3)	85.02 (3)
$^2P_{1/2} - ^2S_{1/2}$	119.62 (8)F	113.04 (6)F	106.98 (5)FH	101.30 (6a)	95.95 (7a)
$^2P_{3/2} - ^2S_{1/2}$	125.38 (8b1)	119.76 (2)	114.72 (1)	110.08 (6a)	105.88 (1)
$^2D_{3/2} - ^2D_{3/2}$	125.51 (10a)B	117.74 (8)BD	110.63 (8)BH	104.14 (9)B	98.16 (10)B
$^2D_{5/2} - ^2D_{5/2}$	128.10 (11)B	120.46 (10a)BD	113.34 (10a)BH	106.76 (10)B	100.60 (10)B
$^4S_{3/2} - ^4P_{1/2}$	136.52 (7)B	127.28 (7a)B	118.66 (8b1)BGH	110.71 (8b1)B	103.31 (6a)A
$^4S_{3/2} - ^4P_{3/2}$	139.87 (11)B	130.59 (8)BD	121.83 (7)BH	113.70 (9a)B	106.04 (11b1)B
$^4S_{3/2} - ^4P_{5/2}$	149.80 (10a)	141.03 (10a)BD	132.85 (10b1)BH	125.15 (9b1)B	117.91 (10b1)B
$^2P_{1/2} - ^2D_{3/2}$	143.53 (4a)	135.33 (2)	127.86 (1)	120.91 (2)	114.45 (6b1)
$^2P_{3/2} - ^2D_{5/2}$	149.94 (8a)B	142.68 (4)BD	136.06 (3a)H	130.02 (5a)	124.48 (3)
$2s2p^4 - 2p^5$					
$^4P_{3/2} - ^2P_{1/2}$			80.59 (1)	75.90 (2b1)	71.54 (1)
$^4P_{5/2} - ^2P_{3/2}$	93.36 (2a)	88.08 (1)	83.23 (4b1)	78.71 (2)	74.49 (2a)
$^4P_{3/2} - ^2P_{3/2}$		92.71 (1)	88.24 (1)	84.03 (1)	80.16 (1)
$^2D_{3/2} - ^2P_{1/2}$	112.27 (6)CE	104.90 (4)C	98.09 (4)CH	91.76 (4)	85.86 (4)
$^2D_{3/2} - ^2P_{3/2}$	122.56 (5)C	115.84 (3)C	109.66 (4a)CH	103.93 (4)	98.58 (5)
$^2D_{5/2} - ^2P_{3/2}$	123.87 (9)CE	117.41 (6)C	111.60 (6)CH	106.23 (8b1)C	101.31 (7)
$^2P_{3/2} - ^2P_{1/2}$	140.82b(6a)	130.97 (4)	122.00 (3a)H	113.76 (6a)	106.16 (5a)
$^2P_{1/2} - ^2P_{1/2}$	155.46 (5)	146.57 (3)	138.49 (2)H	131.09 (3)	124.31 (4)
$^2P_{3/2} - ^2P_{3/2}$	157.40 (8)	148.48 (5)	140.44 (4)H	133.06 (6)	126.32 (6)
$^2S_{1/2} - ^2P_{3/2}$	147.79 (3)	139.36 (2)	131.70 (2)H	124.67 (3)	118.21 (3)

TABLE 4. CLASSIFICATIONS OF LINES ISOELECTRONIC WITH NITROGEN I continued

Wavelengths given in Å.

Relative line intensities listed in brackets after each wavelength.

a indicates possible spurious line intensity due to blending.

bl denotes blend.

b : indicates that wavelength given is calculated from term scheme.

Capital letters refer to previous identifications.

A - Breton et al.(1979); identification in tokamak spectra.

B - Doschek et al.(1974)

C - Doschek et al.(1975b)

D - Fawcett et al.(1974)

E - Fawcett and Hayes (1975)

F - Feldman et al.(1975)

G - Kastner et al.(1974); tentative identification in solar flare spectra.

H - Kononov et al.(1976a).

TABLE 5. CLASSIFICATIONS OF LINES ISOELECTRONIC WITH CARBON I

Transition	Cr XIX	Mn XX	Fe XXI	Co XXII	Ni XXIII
$2s^2 2p^2 - 2s2p^3$					
$^3P_1 - ^1P_1$	95.88 (3)	89.85 (2)	84.26 (1)	78.98 (2b1)	74.07 (2a)
$^3P_0 - ^3S_1$	104.18 (6)D	97.51 (3)D	91.28 (3)DF	85.43 (5b1)	79.99 (2)
$^3P_1 - ^3S_1$	109.64 (8)CD	103.53 (5)D	97.88 (5)DF	92.61 (6)D	87.66 (6a)
$^3P_2 - ^3S_1$	113.97 (10b1)CD	107.89 (8)D	102.22 (7b1)DF	96.88 (8a)D	91.83 (7)D
$^1D_2 - ^1P_1$	110.37 (9a)CD	104.13 (9b1)D	98.36 (9b1)D	93.02 (10b1)	88.11 (5a)
$^3P_2 - ^1D_2$	111.88 (5)	105.24 (3)	99.08 (3)	93.12 (4a)	87.50 (4b1)
$^3P_0 - ^3P_1$	125.93 (4)	116.70 (2)	108.12 (2)	100.14 (2)	92.75 (2)
$^3P_1 - ^3P_2$	132.11 (2)	123.30 (6a)	115.15 (4a)F	107.58 (3a)	100.50b(3a)
$^3P_1 - ^3P_1$	133.99 (9)	125.42 (6a)	117.51 (6b1)	110.14 (5a)	103.23 (6a)
$^3P_1 - ^3P_0$	134.89 (5)	126.46 (3)	118.69 (8b1)F	111.47 (4a)	104.70 (3a)
$^3P_2 - ^3P_2$	138.45 (10)CD	129.55 (8)D	121.21 (8)DF	113.37 (9a)	106.02 (11b1)
$^3P_2 - ^3P_1$	140.51 (3)	131.88b(2a)	123.83b(1)E	116.22 (1)	109.06 (2b1)
$^1S_0 - ^1P_1$	126.30 (11b1)	119.12 (4)	112.47 (4)F	106.23 (8b1)	100.42 (5a)
$^1D_2 - ^1D_2$	126.33 (11b1)CD	119.54 (9)D	113.30 (10a)DF	107.49 (10a)D	102.08 (10b1)D
$^3P_0 - ^3D_1$	148.64 (6)	138.30 (3)	128.73 (5)BF	119.92 (5)	111.86 (8a)A
$^3P_1 - ^3D_1$	160.01 (2)	150.71 (2a)	142.27 (1)	134.57 (1)	127.46 (1)
$^3P_1 - ^3D_2$	160.30 (7)C	150.80 (5)	142.16 (6a)F	134.13 (5)	126.54 (6)
$^3P_2 - ^3D_3$	165.46 (7)C	155.21 (4)	145.65 (4)F	136.75 (5)	128.30 (6)
$^3P_2 - ^3D_2$	169.73 (1)		151.50 FN		
$2s2p^3 - 2p^4$					
$^5S_2 - ^3P_2$	95.62 (2)	90.76 (1)	86.26 (1)	82.09 (1)	78.21 (1)
$^3D_3 - ^1D_2$	111.18 (4)	104.67 (2)	98.69 (3)	93.00 (10b1)	87.77 (2a)
$^3D_1 - ^3P_0$	118.31 (6)	111.01 (6b1)	104.29 (3)	98.07 (2)	92.32 (2)
$^3D_2 - ^3P_1$	118.67 (7)C	111.00 (6b1)	103.83 (4a)	97.16 (5a)	90.96 (2)
$^3D_1 - ^3P_1$	118.83 (6)	111.04 (6b1)	103.77 (3a)	96.93 (8a)	90.49 (3)
$^3D_2 - ^3P_2$	128.43 (11b1)	121.49 (5a)	115.08 (3a)	109.14 (9b1)	103.87 (4a)
$^3D_1 - ^3P_2$	128.63 (3)	121.55 (4a)	115.01 (2a)	108.84 (2)	103.07 (2)
$^3D_3 - ^3P_2$	130.99 (9)C	124.56 (6)	118.71 (8b1)	113.24 (8a)	108.27 (7)
$^3P_2 - ^1D_2$	127.95 (1)	120.82 (1)	114.30 (1)	108.16 (3a)	102.50 (1)
$^3P_0 - ^3P_1$	137.89 (2)	129.31 (2)	121.36 (1)	113.93 (2a)	107.00b(1)
$^3P_1 - ^3P_0$	138.15 (4)	130.38 (2)	123.33 (2)	116.97 (1)	111.23b(5a)
$^3P_1 - ^3P_1$	138.86 (1)				
$^3P_2 - ^3P_1$	140.92 (6)	132.79 (4a)	125.29 (3)	118.31 (4)	111.78b(5a)
$^3P_1 - ^3P_2$	152.42 (3)	145.16 (2)	138.61 (1)	132.63 (2)	127.21 (2)
$^3P_2 - ^3P_2$	154.92 (3)	148.10 (1)	142.05 (5a)	136.56b(6a)	131.60 (2)
$^1P_1 - ^1S_0$	143.57 (6a)	135.06 (3)	127.04 (3)	119.55 (4)	112.55 (3)

TABLE 5. CLASSIFICATIONS OF LINES ISOELECTRONIC WITH CARBON I continued

Transition	Cr XIX	Mn XX	Fe XXI	Co XXII	Ni XXIII
$^1D_2-^1D_2$	163.94 (9)	153.98 (5)	144.79 (6a)F	136.49 (8a)	128.67 (8bl)
$^3S_1-^3P_0$	179.18 (4bl)	167.12 (2a)	156.21 (1)	146.40 (1)	137.55 (2)
$^3S_1-^3P_1$	180.37 (3)	167.19 (2a)	155.06 (2)	143.87(3bl)	133.54 (3)
$^3S_1-^3P_2$	203.94b(10a)	192.20 (1)	181.57 (1)	171.79 (2)	
$^1P_1-^1D_2$	201.82 (2)	190.23 (1)		170.09 (2)	

Wavelengths given in Å.
Relative line intensities listed in brackets after each wavelength.
a indicates possible spurious line intensity due to blending.
bl denotes blend.
b indicates that wavelength given is calculated from term scheme.
N means that line is not observed in present spectra
Other capital letters refer to previous identifications.
A - Breton et al.(1979); identification in tokamak spectra
B - Fawcett and Cowan (1975); identification in solar flare spectra
C - Fawcett and Hayes (1975)
D - Feldman et al.(1975)
E - Kastner et al.(1974); identification in solar flare spectra
F - Kononov et al.(1976a)

TABLE 6. CLASSIFICATIONS OF LINES ISOELECTRONIC WITH BORON I

Transition	Cr XX	Mn XXI	Fe XXII	Co XXIII	Ni XXIV
$2s^2 2p - 2s 2p^2$					
$^2P_{\frac{1}{2}} - ^2P_{3/2}$	116.05 (5)B	108.14 (4)B	100.78 (4)BF	93.90 (3)	87.50 (4bl)
$^2P_{\frac{1}{2}} - ^2P_{\frac{1}{2}}$	117.95 (3)	109.78 (2)	102.23 (7bl)F	95.16 (1)	88.54 (1)
$^2P_{3/2} - ^2P_{3/2}$	128.42 (11bl)BD	121.16 (9)B	114.41 (8)BCF	108.03 (10a)B	102.11 (10bl)B
$^2P_{3/2} - ^2P_{\frac{1}{2}}$	130.76 (9)D	123.23 (6a)	116.28 (6)F	109.70 (6)	103.53 (6a)
$^2P_{\frac{1}{2}} - ^2S_{\frac{1}{2}}$	131.50 (9)A	124.08 (7)	117.17 (7)EF	110.71 (8bl)	104.64 (6a)A
$^2P_{3/2} - ^2S_{\frac{1}{2}}$	147.62 (1)	141.53b(3a)	136.01 (3a)		
$^2P_{\frac{1}{2}} - ^2D_{3/2}$	156.00 (8)	145.45 (5)	135.78 (6)EF	126.82 (5)	118.52 (5)
$^2P_{3/2} - ^2D_{5/2}$	175.42 (7bl)	165.34 (4)	155.92 (4)F	147.09 (4)	138.80 (4)
$^2P_{3/2} - ^2D_{3/2}$	179.21 (4bl)		161.74 (1)T		
$2s 2p^2 - 2p^3$					
$^4P_{5/2} - ^2D_{5/2}$	122.29 (2)T	115.69 (2)T	109.53 (3a)T	103.80 (2)T	98.39 (1)T
$^2D_{3/2} - ^2P_{3/2}$	129.26 (4)	120.50 (10a)	112.21 (2)	104.45 (2)	97.17 (6a)
$^2D_{5/2} - ^2P_{3/2}$	131.31 (7)	122.97 (4)	115.19 (4a)	107.31 (4)	101.13 (2)
$^2D_{3/2} - ^2P_{\frac{1}{2}}$	135.26 (6)	127.36 (7a)	120.03 (8bl)	113.17 (5a)	106.68 (3)
$^4P_{\frac{1}{2}} - ^4S_{3/2}$	133.82 (7)	125.35 (5a)	117.52 (6bl)F	110.23 (4a)	103.43 (9bl)
$^4P_{3/2} - ^4S_{3/2}$	140.75 (9a)	132.90 (6a)	125.71 (6)F	119.12 (5)	113.14 (4)
$^4P_{5/2} - ^4S_{3/2}$	148.99 (9)	141.49 (6a)	134.65 (6)F	128.37 (6)	122.72 (5)
$^2S_{\frac{1}{2}} - ^2P_{3/2}$	152.86 (3)	140.55 (2)	129.17 (1)	118.68 (1)	109.03 (2bl)
$^2S_{\frac{1}{2}} - ^2P_{\frac{1}{2}}$	161.33 (2)	149.97b(3a)	139.64 (1)	130.06b(2a)	121.15 (1)
$^2D_{3/2} - ^2D_{5/2}$	164.63 (4)	154.43 (3)	144.85 (6a)F	136.12 (3a)	127.78 (2)
$^2D_{5/2} - ^2D_{5/2}$	167.97 (8)	158.51 (5)	149.87 (5)F	142.05 (5)	134.73 (4)
$^2D_{3/2} - ^2D_{3/2}$	169.87 (5)	160.42 (3)	151.54 (3)	143.30 (3)	135.47 (2)
$^2D_{5/2} - ^2D_{3/2}$	173.42 (4)	164.83 (3a)	157.03 (4a)	149.88 (2)	143.30 (2)
$^2P_{\frac{1}{2}} - ^2P_{3/2}$	176.42 (1)	164.87 (2a)	153.96 (1)	143.89 (3bl)	134.53 (2)
$^2P_{3/2} - ^2P_{3/2}$	180.85 (5)	168.72 (4a)	157.37 (4)F	146.86 (5a)	137.01 (2)
$^2P_{\frac{1}{2}} - ^2P_{\frac{1}{2}}$	187.79 (3)	177.99 (3)	169.08 (1)	160.97 (2)	
$^2P_{3/2} - ^2P_{\frac{1}{2}}$	192.82 (1)	182.48 (2)	173.21 (1)		
$^2S_{\frac{1}{2}} - ^2D_{3/2}$	213.10 (4a)	198.04 (2a)		171.50b(1)	159.69 (1)
$^2P_{3/2} - ^2D_{5/2}$	258.57b(4a)	243.69 (1)			
$^2P_{3/2} - ^2D_{3/2}$	271.72 (2)	258.95 (2a)T			

Wavelengths given in Å.
Relative line intensities listed in brackets after each wavelength.
a indicates possible spurious line intensity due to blending.
bl denotes blend.
b indicates that wavelength given is calculated from term scheme.
T follows wavelength of tentative identification.
Other capital letters refer to previous identifications.
A - Breton et al. (1979); identifications in tokamak spectra
B - Doschek et al. (1975a)
C - Fawcett and Cowan (1975); identification in solar flare spectra
D - Fawcett and Hayes (1975)
E - Kastner et al. (1974); identifications in solar flare spectra
F - Kononov et al. (1976a)

TABLE 7. CLASSIFICATIONS OF LINES ISOELECTRONIC WITH BERYLLIUM I

Transition	Cr XXI	Mn XXII	Fe XXIII	Co XXIV	Ni XXV
$2s^2$-2s2p					
$^1S_0$-$^1P_1$	149.87 (10a)A	141.09 (10a)	132.84 (10b1)B	125.15 (9b1)	117.91 (10b1)
2s2p-$2p^2$					
$^3P_2$-$^1D_2$	154.61 (4)	145.27 (3)	136.53 (4)	128.24 (4)	120.53 (3)
$^3P_1$-$^3P_2$	165.03 (5)	154.28 (4)	144.36 (4)	135.24 (4)	126.73 (3)
$^3P_0$-$^3P_1$	168.62 (4)	157.58 (4)	147.24 (3)	137.73 (3)	128.85 (8b1)
$^3P_1$-$^3P_1$	175.45 (7b1)	164.48 (3)	154.27 (2)	144.83 (2)	135.95 (2)
$^3P_2$-$^3P_2$	184.48 (6)	175.18 (5)	166.74 (4)	159.00 (4a)	151.90 (3)
$^3P_1$-$^3P_0$	190.98 (4)	181.69 (2)	173.31 (2a)	165.75 (1)	158.84 (1)T
$^3P_2$-$^3P_1$	197.61 (2)	188.45 (4)	180.10 (1)	172.42b(10a)	165.36 (2a)
$^1P_1$-$^1S_0$	170.16 (4)	159.33 (4a)	149.22 (3)	139.80 (3)	130.99 (2)
$^1P_1$-$^1D_2$	259.97 (2)	239.87 (1)	221.33 (5b1)	204.10 (1)	188.13 (2)

Wavelengths given in Å.
Relative line intensities listed in brackets after each wavelength.
a indicates possible spurious line intensity due to blending.
bl denotes blend.
b indicates that wavelength given is calculated from term scheme.
T follows wavelength of tentative identification.
Other capital letters refer to previous identifications.
A - Breton et al.(1979); identification in tokamak spectra.
B - Kastner et al.(1974); identification in solar flare spectra.

TABLE 8. CLASSIFICATIONS OF LINES ISOELECTRONIC WITH LITHIUM I

Transition	Cr XXII	Mn XXIII	Fe XXIV	Co XXV	Ni XXVI
2s - 2p					
$^2S_{\frac{1}{2}}-^2P_{3/2}$	222.98 (3)AB	206.89 (3a)AB	191.99 (4a)AB	178.20 NP	165.42 NTA
$^2S_{\frac{1}{2}}-^2P_{\frac{1}{2}}$	279.74 (6b1)AB	266.89 (1)AB	255.10 NAB	244.25 NP	234.20 NAB

Wavelengths given in Å.
Relative line intensities listed in brackets after each wavelength.
a indicates possible spurious line intensity due to blending.
b1 denotes blend.
N indicates that line is not observed in present spectra.
P refers to wavelengths predicted by isoelectronic interpolation.
T follows wavelength of tentative identification.
Other capital letters refer to previous identifications.
A - Sandlin et al. (1976)) identifications in
B - Widing and Purcell (1976)) solar flare spectra

TABLE 9. ENERGY LEVELS ISOELECTRONIC WITH FLUORINE I

Level	Cr XVI	Mn XVII	Fe XVIII	Co XIX	Ni XX
$2s^2 2p^5$					
$^2P_{3/2}$	0	0	0	0	0
$^2P_{\frac{1}{2}}$	70,830	85,510	102,620	121,960	144,040
$2s2p^6$					
$^2S_{\frac{1}{2}}$	937,910	1,000,000	1,064,620	1,131,860	1,202,360

Energies given in cm^{-1}.

TABLE 10. ENERGY LEVELS ISOELECTRONIC WITH OXYGEN I

Level	Cr XVII	Mn XVIII	Fe XIX	Co XX	Ni XXI
$2s^2 2p^4$					
$^3P_2$	0	0	0	0	0
$^3P_0$	58,150	66,580	75,350	83,930	92,840
$^3P_1$	60,380	73,590	89,430	107,410	128,290
$^1D_2$	135,160	150,640	168,770	189,300	212,230
$^1S_0$	263,180	292,070	325,100	363,240	406,820
$2s2p^5$					
$^3P_2$	813,600	866,700	922,760	981,550	1,043,300
$^3P_1$	858,150	919,460	984,690	1,053,300	1,126,000
$^3P_0$	887,920	956,220	1,029,900	1,108,510	1,193,140
$^1P_1$	1,116,420	1,189,820	1,267,430	1,349,530	1,436,370
$2p^6$					
$^1S_0$	1,886,950	2,007,550	2,133,830	2,265,780	2,403,490

Energies given in cm^{-1}.

TABLE 11. ENERGY LEVELS ISOELECTRONIC WITH NITROGEN I

Level	Cr XVIII	Mn XIX	Fe XX	Co XXI	Ni XXII
$2s^2 2p^3$					
$^4S_{3/2}$	0	0	0	0	0
$^2D_{3/2}$	126,040	131,820	138,270	147,080	157,480
$^2D_{5/2}$	150,800	162,520	175,810	191,530	209,380
$^2P_{\frac{1}{2}}$	226,100	242,190	260,090	280,260	302,450
$^2P_{3/2}$	264,490	291,800	323,180	359,030	400,120
$2s2p^4$					
$^4P_{5/2}$	667,560	709,070	752,730	799,040	848,100
$^4P_{3/2}$	714,950	765,760	820,820	879,510	943,040
$^4P_{\frac{1}{2}}$	732,490	785,670	842,740	903,260	967,960
$^2D_{3/2}$	922,800	981,120	1,042,210	1,107,330	1,176,180
$^2D_{5/2}$	931,420	992,670	1,058,130	1,128,170	1,203,460
$^2S_{\frac{1}{2}}$	1,062,060	1,126,820	1,194,850	1,267,470	1,344,630
$^2P_{3/2}$	1,103,370	1,170,890	1,242,080	1,318,040	1,398,940
$^2P_{\frac{1}{2}}$	1,170,210	1,252,140	1,339,680	1,434,250	1,536,480
$2p^5$					
$^2P_{3/2}$	1,738,700	1,844,390	1,954,150	2,069,560	2,190,550
$^2P_{\frac{1}{2}}$	1,813,480	1,934,420	2,061,730	2,197,080	2,340,890

Energies given in cm^{-1}.

TABLE 12. ENERGY LEVELS ISOELECTRONIC WITH CARBON 1

Level	Cr XIX	Mn XX	Fe XXI	Co XXII	Ni XXIII
$2s^2 2p^2$					
$^3P_0$	0	0	0	0	0
$^3P_1$	47,770	59,560	73,910	90,750	109,390
$^3P_2$	82,420	98,630	117,300	138,240	161,190
$^1D_2$	184,690	212,260	243,950	281,890	324,460
$^1S_0$	298,990	333,090	371,520	415,540	463,620
$2s2p^3$					
$^5S_2$	404,440	443,970	487,030	534,430	585,620
$^3D_2$	671,590	722,690	777,350	836,320	899,650
$^3D_1$	672,750	723,070	776,810	833,860	893,970
$^3D_3$	686,810	742,930	803,900	869,520	940,610
$^3P_0$	789,100	850,320	916,460	987,840	1,064,460
$^3P_1$	794,120	856,900	924,880	998,650	1,078,110
$^3P_2$	804,690	870,560	942,330	1,020,310	1,104,380
$^3S_1$	959,860	1,025,500	1,095,560	1,170,490	1,250,160
$^1D_2$	976,270	1,048,820	1,126,550	1,212,170	1,304,040
$^1P_1$	1,090,760	1,172,580	1,260,650	1,356,890	1,459,440
$2p^4$					
$^3P_2$	1,450,200	1,545,780	1,646,320	1,752,610	1,864,230
$^3P_1$	1,514,290	1,623,630	1,740,460	1,865,550	1,999,010
$^3P_0$	1,517,960	1,623,890	1,735,720	1,853,540	1,977,150
$^1D_2$	1,586,250	1,698,270	1,817,220	1,944,830	2,079,990
$^1S_0$	1,787,280	1,912,990	2,047,800	2,193,360	2,347,930

Energies given in cm^{-1}.

TABLE 13. ENERGY LEVELS ISOELECTRONIC WITH BORON I

Level	Cr XX	Mn XXI	Fe XXII	Co XXIII	Ni XXIV
$2s^2 2p$					
$^2P_{\frac{1}{2}}$	0	0	0	0	0
$^2P_{3/2}$	83,030	99,360	118,230	139,310	163,570
$2s2p^2$					
$^4P_{\frac{1}{2}}$	354,620+x	379,660+x	405,620+x	431,580+x	457,980+x
$^4P_{3/2}$	391,410+x	424,980+x	461,060+x	499,320+x	540,950+x
$^4P_{5/2}$	430,700+x	470,670+x	513,870+x	559,800+x	609,950+x
$^2D_{3/2}$	641,030	687,540	736,490	788,490	843,710
$^2D_{5/2}$	653,090	704,190	759,590	819,160	884,030
$^2S_{\frac{1}{2}}$	760,460	805,930	853,490	903,250	955,660
$^2P_{\frac{1}{2}}$	847,810	910,880	978,190	1,050,890	1,129,490
$^2P_{3/2}$	861,700	924,710	992,260	1,064,940	1,142,910
$2p^3$					
$^4S_{3/2}$	1,101,890+x	1,177,430+x	1,256,540+x	1,338,780+x	1,424,810+x
$^2D_{3/2}$	1,229,720	1,310,890	1,396,400	1,486,340	1,581,860
$^2D_{5/2}$	1,248,440	1,335,070	1,426,850	1,523,160	1,626,280
$^2P_{\frac{1}{2}}$	1,380,320	1,472,710	1,569,610	1,672,110	1,781,090
$^2P_{3/2}$	1,414,650	1,517,410	1,627,690	1,745,850	1,872,810

Energies given in cm^{-1}.
x indicates possible error due to tentative identification.

TABLE 14. ENERGY LEVELS ISOELECTRONIC WITH BERYLLIUM I

Level	Cr XXI	MN XXII	Fe XXIII	Co XXIV	Ni XXV
$2s^2$					
$^1S_0$	0	0	0	0	0
2s2p					
$^3P_0$	318,100	333,340	348,210	363,160	378,630
$^3P_1$	341,180	359,970	379,160	398,740	419,190
$^3P_2$	405,090	437,290	472,130	509,240	549,980
$^1P_1$	667,230	708,770	752,760	799,040	848,100
$2p^2$					
$^3P_0$	864,800	910,360	956,160	1,002,060	1,048,750+x
$^3P_1$	911,150	967,940	1,027,370	1,089,210	1,154,730
$^3P_2$	947,140	1,008,130	1,071,870	1,138,180	1,208,290
$^1D_2$	1,051,890	1,125,660	1,204,570	1,289,000	1,379,650
$^1S_0$	1,254,910	1,336,400	1,422,910	1,514,340	1,611,520

Energies given in cm^{-1}.
x indicates possible error due to tentative identification.

TABLE 15. ENERGY LEVELS ISOELECTRONIC WITH LITHIUM I

Level	Cr XXII	Mn XXIII	Fe XXIV	Co XXV	Ni XXVI
2s					
$^2S_{\frac{1}{2}}$	0	0	0	0	0
2p					
$^2P_{\frac{1}{2}}$	357,470	374,690	392,000	409,420+x	426,990
$^2P_{3/2}$	448,470	483,350	520,860	561,160+x	604,520+x

Energies given in cm^{-1}.
x indicates possible error due to predictions and tentative identification.

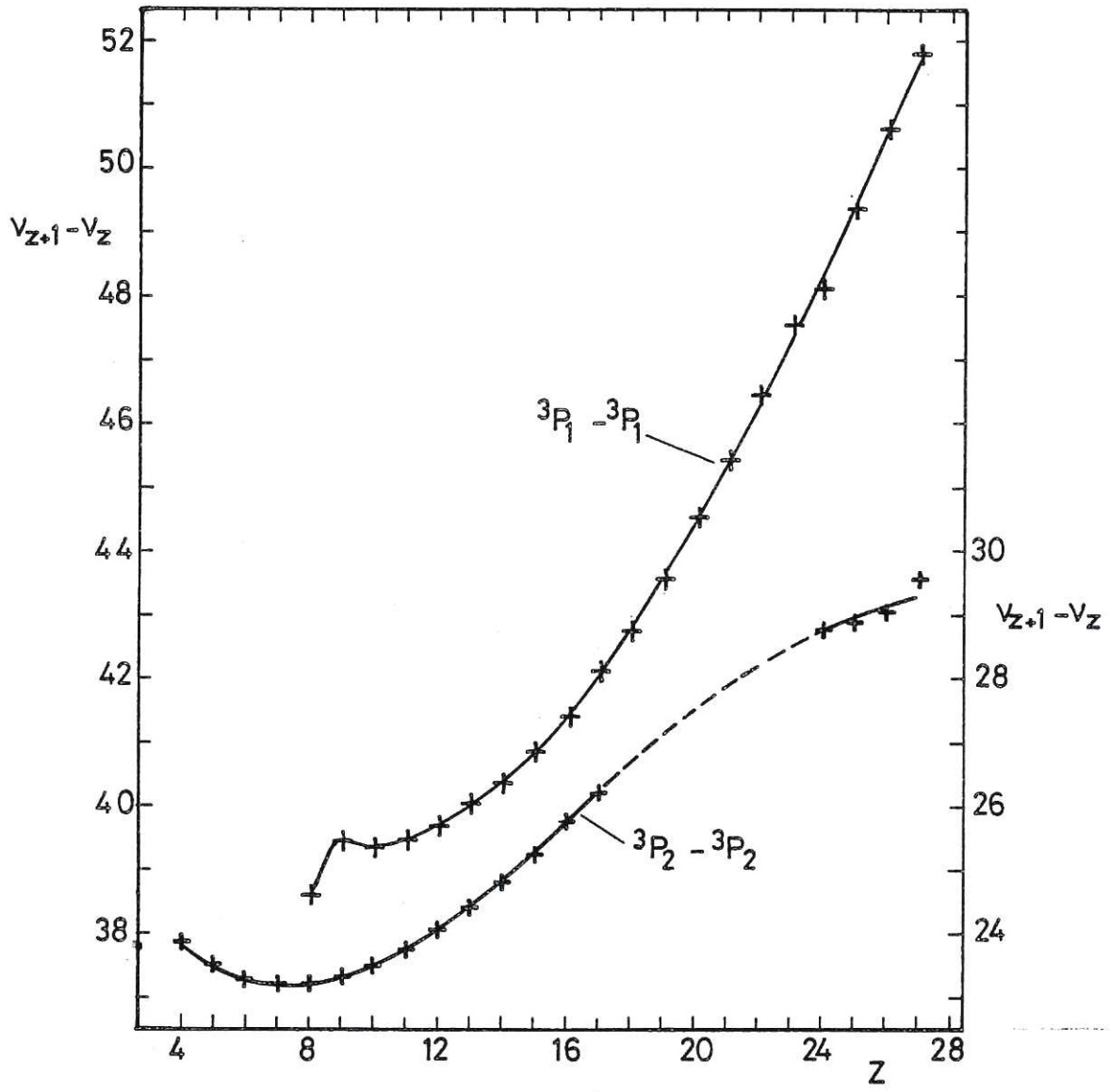

Fig.3 Extrapolation curves for the $2s^2 2p^4\ ^3P_1 - 2s\,2p^5\ ^3P_1$ and $2s\,2p^3 P_2 - 2p^2\ ^3P_2$ transitions.

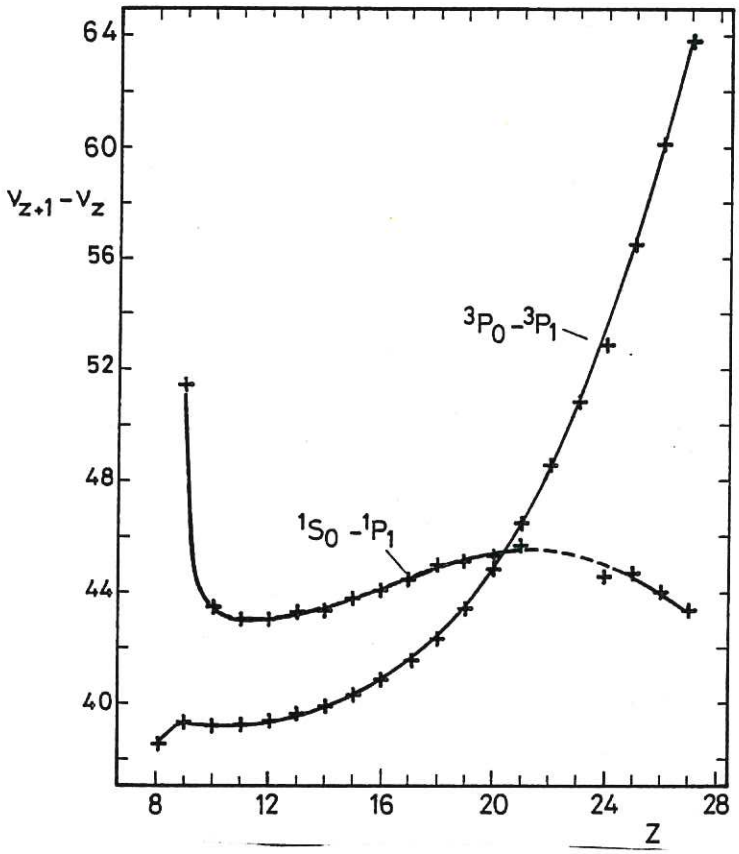

Fig.4 Extrapolation curves for the $2s^2\ 2p^4\ ^3P_0 - 2s\,2p^5\ ^3P_1$ and $2s^2\ 2p^4\ ^1S_0 - 2s\,2p^5\ ^1P_1$ transition.

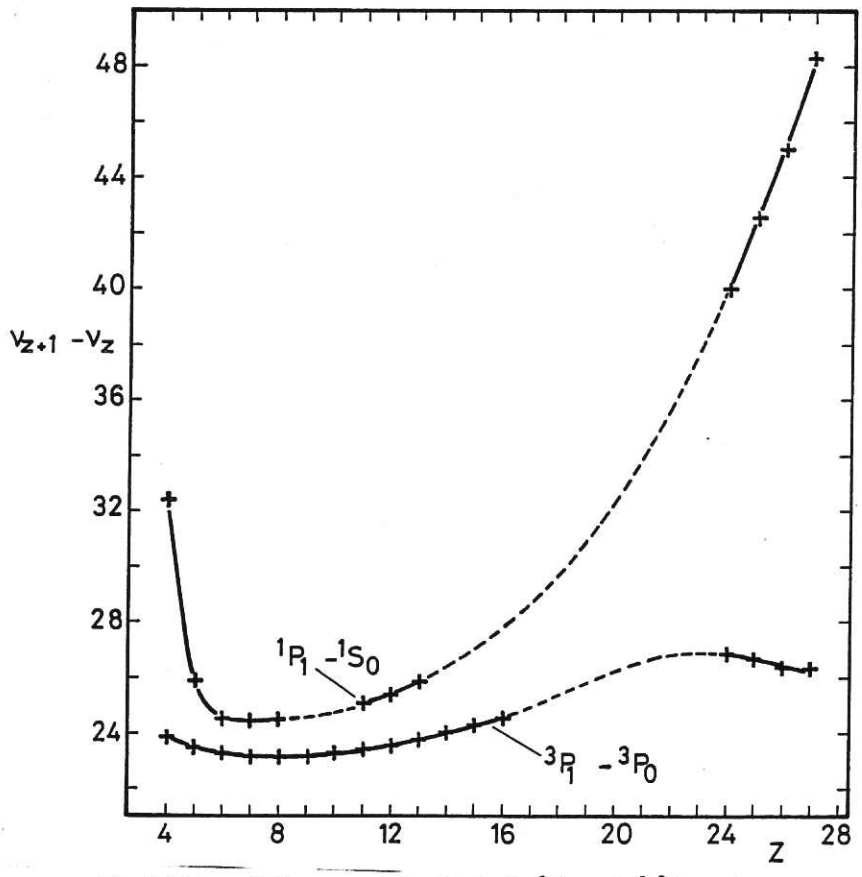

Fig.5 Extrapolation curves for the $2s\,2p\ ^3P_1 - 2p^2\ ^3P_0$ and $2s\,2p\ ^1P_1 - 2p^2\ ^1S_0$ transitions.

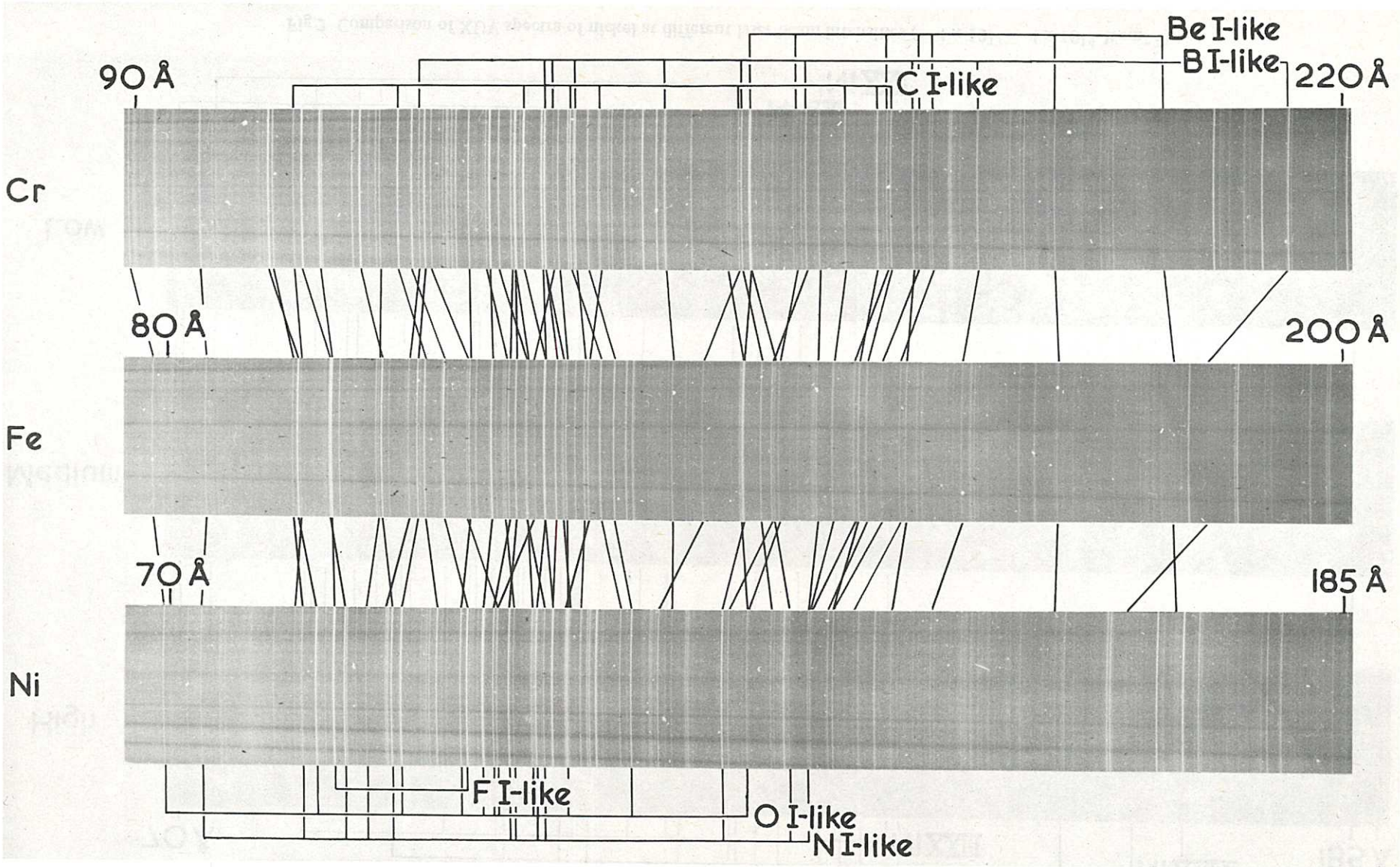

Fig.1 XUV spectra of chromium, iron and nickel at high laser beam intensity ($\sim 4 \times 10^{14}$ Wcm^{-2}).

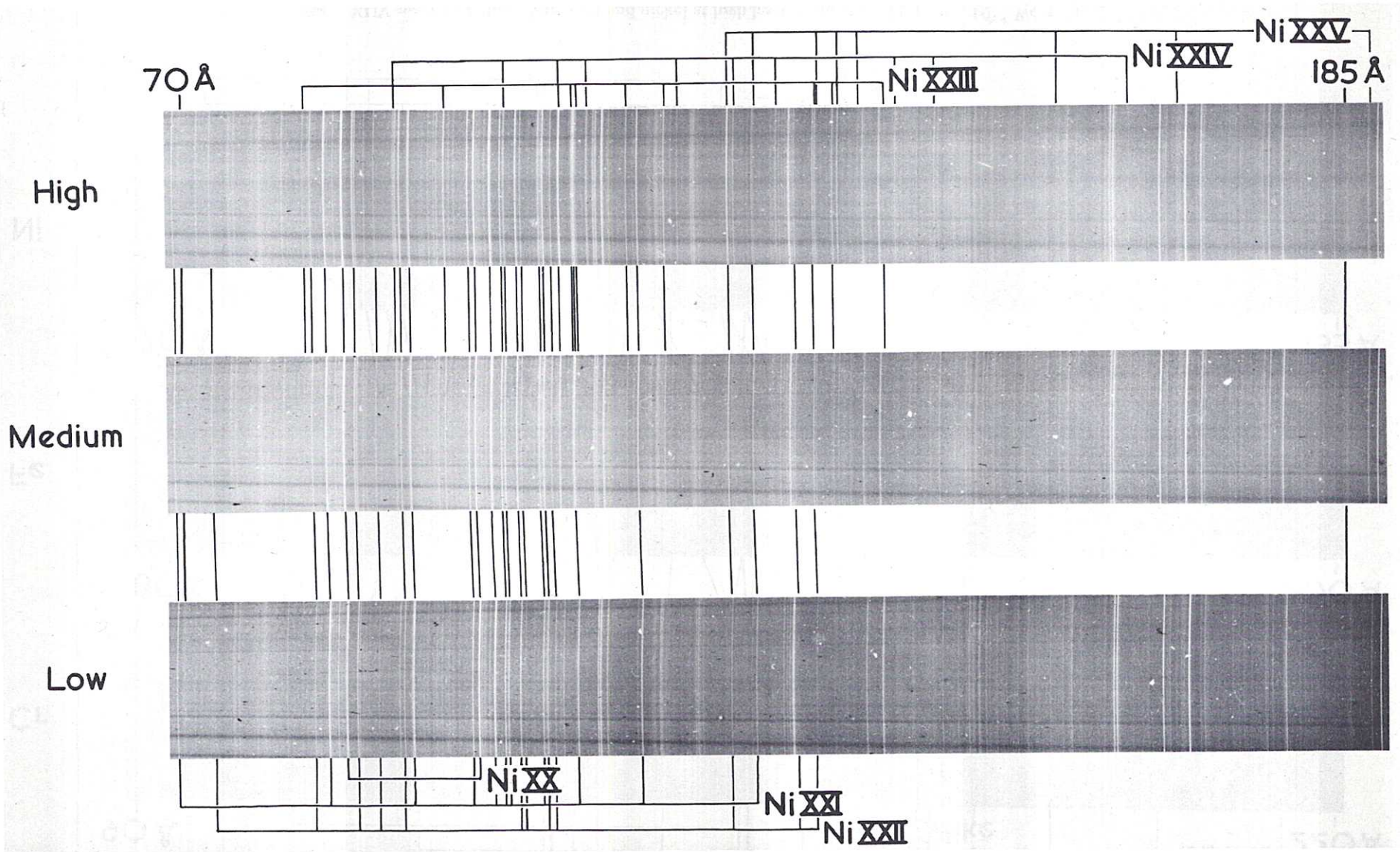

Fig.2 Comparison of XUV spectra of nickel at different laser beam intensities ($\sim 4 \times 10^{13} - 4 \times 10^{14}$ Wcm^{-2}).

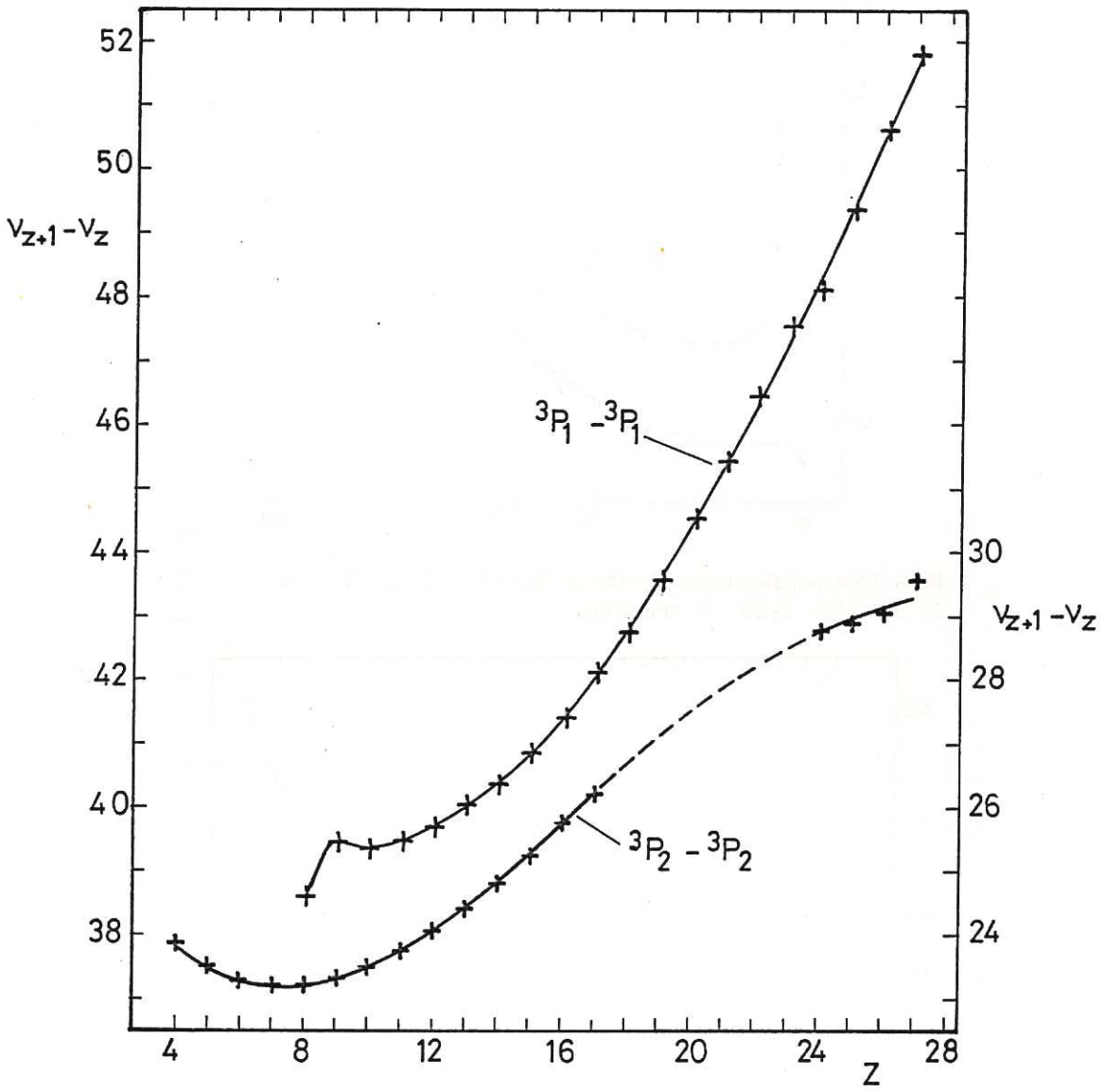

Fig.3 Extrapolation curves for the $2s^2 2p^4\ ^3P_1 - 2s\,2p^5\ ^3P_1$ and $2s\,2p^3\ ^3P_2 - 2p^2\ ^3P_2$ transitions.

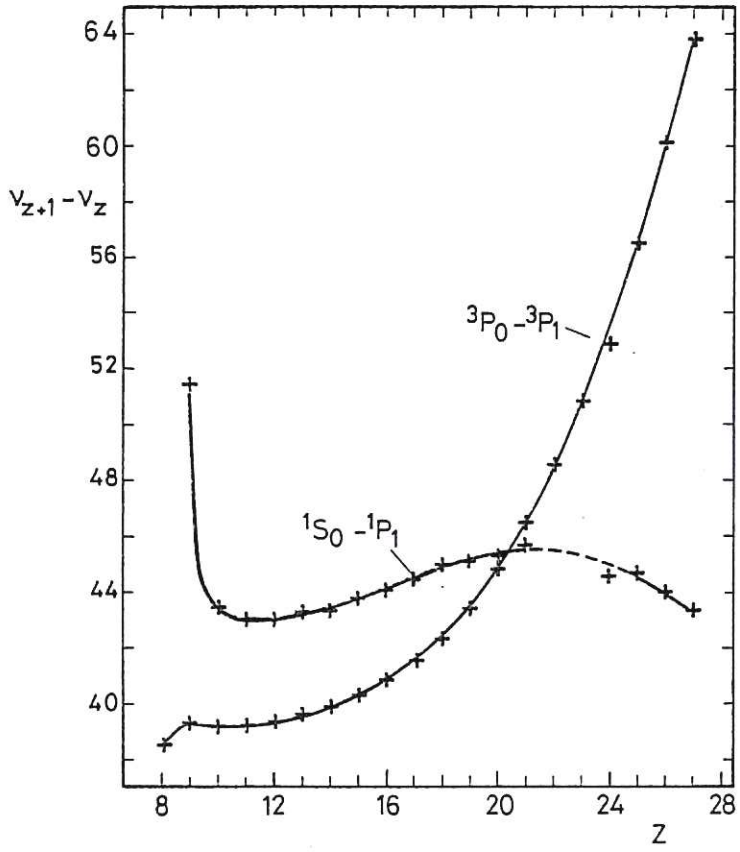

Fig.4 Extrapolation curves for the $2s^2\ 2p^4\ ^3P_0 - 2s\,2p^5\ ^3P_1$ and $2s^2\ 2p^4\ ^1S_0 - 2s\,2p^5\ ^1P_1$ transition.

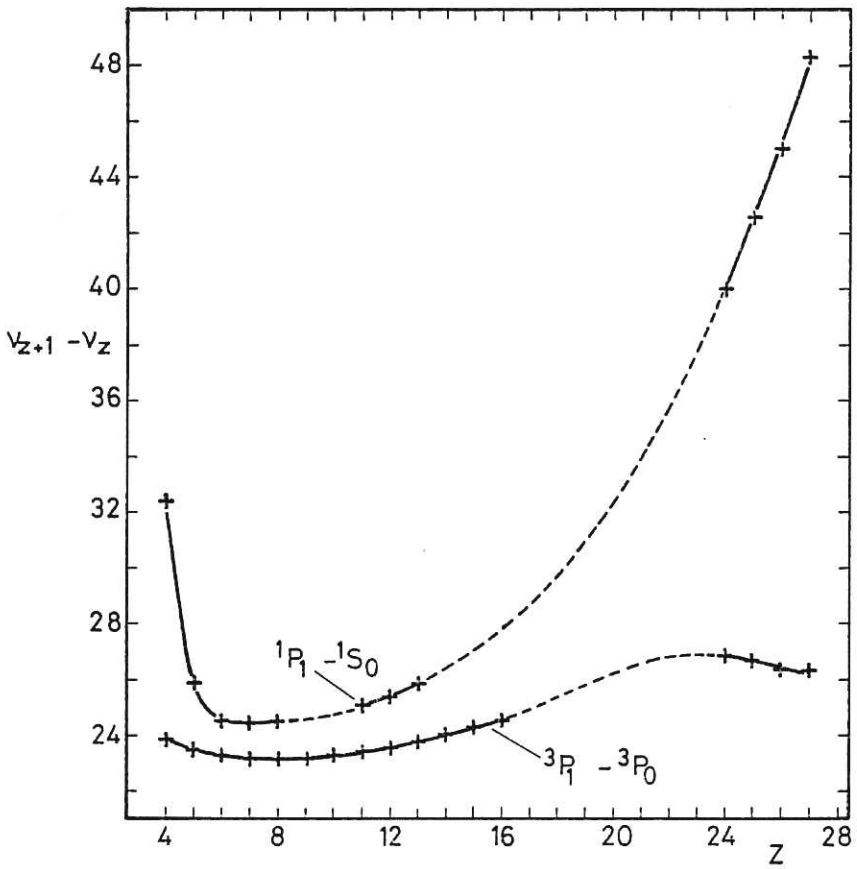

Fig.5 Extrapolation curves for the $2s\,2p\ ^3P_1 - 2p^2\ ^3P_0$ and $2s\,2p\ ^1P_1 - 2p^2\ ^1S_0$ transitions.